Electro-Rheological Response of Liquid Crystals under Oscillatory Squeeze Flow*

Takatsune NARUMI**, Howard SEE***, Yasuhiro YAMAGUCHI** and Tomiichi HASEGAWA**

We have investigated the electro-rheological (ER) properties of liquid crystals in an oscillatory squeezing flow. A Micro Fourier Rheometer was utilized to estimate the complex viscosity and phase shift. A clear dip in the phase angle was observed, centred around a frequency which increased with electric field strength. It was found that this critical frequency was proportional to the inverse of the response time required for the liquid crystal molecules to align under the electric field. Similar ER effects to those observed under steady shearing were obtained in the oscillatory flow, but the ER effect at high frequency is smaller than that under no electric field. In other words, a negative ER effect was obtained under low electric fields. A rheological model for the dynamic response was obtained through the control theory and the transfer function thus derived will be useful for estimating the output response in a flow or motion control system.

Key Words: Electro-Rheological Fluid, Liquid Crystal, Squeeze Flow, Oscillatory Flow, Non-Newtonian Fluid, Flow Control

1. Introduction

An electro-rheological (ER) fluid is an example of a so-called "smart fluid", which shows a dramatic but reversible increase in flow resistance when placed under an electric field (E). The tunable flow properties of these materials lend them to a variety of engineering applications, such as adjustable vibration damping devices, and they have been the focus of intense research and development efforts in recent years around the world. Broadly speaking, there are two main types of electro-rheological fluids: particulate types and homogeneous types. The particulate types are essentially dispersions of micron-sized, semi-conducting particles in an insulating carrier liquid: The application of the electric field causes the particles to polarize electrically, and the resulting electrostatic interaction forces between the particles lead to the formation of elongated aggregates in the field direction which in turn causes the viscosity to increase (review articles on these systems are available [e.g. (1)–(3)]). On the other hand, homogenous ER fluids are continuous materials which respond mechanically under an electric field: the best known examples are liquid crystals, where the ER properties under steady shear flow as well as some applications have been reported for monomer type[(4)–(6)] and polymer type liquid crystals[(7)–(9)]. In addition, although not strictly homogeneous, other types of ER fluids based on liquid crystals have also been tested; examples include immiscible blends of polymers and liquid crystalline systems[(10)–(12)]. Although in general the homogeneous types, in particular the monomer type liquid crystals, are not able to produce viscosity increases as large as the particulate types, they do have the advantage that they are less susceptible to particle-related problems such sedimentation and colloidal instability. Further, since their structural units are on a molecular scale, the homogeneous fluids have enormous potential usage in very small mechanical devices (e.g. in 'micro-machines'). In addition, the polymer types or immiscible blends show higher ER effects than the monomer type, but there are difficulties in applying them to micro channels because of their high viscosity. Since the inertia effect becomes negligible in micro devices, the monomer type liquid crystal, in fact, becomes very useful as an ER fluid, even though it does not have so high an ER effect.

The majority of experimental studies on electro-rheological materials reported to date have used steady

* Received 20th December, 2004 (No. 04-4262)

** Department of Mechanical and Production Engineering, Faculty of Engineering, Niigata University, 8050 2-no-cho, Ikarashi, Niigata 950–2181, Japan.
E-mail: narumi@eng.niigata-u.ac.jp

*** Department of Chemical Engineering, Faculty of Engineering, University of Sydney, Sydney, NSW 2006, Australia

shear flow to characterize the field-induced increase in flow resistance. A few studies have attempted to further probe the mechanical properties under various electric fields by applying small amplitude oscillatory shear flow to determine the linear viscoelastic functions e.g. the complex moduli or complex viscosity η^* ($\eta^* = \eta' - i\eta''$). For example, Klingenberg and co-workers[13]-[15] have examined the linear viscoelastic behaviour of a particulate electro-rheological fluid (alumina particles dispersed in poly (dimethyl siloxane)). They found that there was a dramatic increase in stiffness as electric field strength was raised – indeed, it was found that both the storage and loss moduli scaled as E^2. Further, when investigating the dependence on the oscillation frequency (ω), it was found that good data collapse could be obtained if the frequency axis was re-plotted using the parameter ω/E^2. This scaling behaviour is in agreement with predictions from a particle-level computer simulation.

Flow geometries more complex than simple shearing have been used by a few researchers to explore electro-rheological behaviour. Examining the behaviour in flow fields other than simple shearing is useful because many industrial applications involve quite complex flow geometries. Particularly relevant to this study are the reports which have used squeeze flow to characterise electro-rheological materials. For example, See et al.[16] used oscillatory squeeze flow to probe the response of a particulate-type fluid. In this experiment, the sample was sandwiched between two parallel electrodes, and the gap was changed sinusoidally about a mean value. The force waveforms revealed much about the process of break-up and reformation of the aggregate structures in the activated material. Further, from an engineering perspective, El Wahed and co-workers[17]-[19] have extensively explored the performance of particulate-type fluids in dynamic squeeze flow, with a focus on the potential application in vibration isolation devices. Particle-level computer simulations have also been carried out to investigate structural changes during squeeze flow under constant approach speeds[20].

The studies described above, which have employed small amplitude oscillations and/or squeeze flow, have all focused on the particulate electro-rheological systems. To the best of our knowledge, there have been no reports of the use of these techniques to characterize a homogeneous liquid crystalline electro-rheological fluid, despite the potential importance of these fluids in many engineering applications. This paper will present studies we have carried out on liquid crystals under small amplitude oscillatory squeeze flow, where we have examined in particular the dependence of the viscoelastic functions on the electric field strength and oscillation frequency.

Previous studies of the electrorheology of monomer type liquid crystals have mainly focused on the behaviour under steady shearing, and have examined the field-dependent viscosity or steady shear stress[4],[5],[21],[22]. Further, there have been reports of the effect on the steady shear viscosity of temperature[23]. The mechanism behind the field-induced viscosity increase in liquid crystals is thought to be that the individual liquid crystal molecules possess a dipole moment, and this tends to align in the electric field direction (as illustrated schematically in Fig. 1). This alignment of the axis of the liquid crystal system (the "director" axis) so that it is perpendicular to the flow direction is the reason for the increased viscosity. This viscosity change can also be expressed through the Miesowicz viscosities[24]. Theoretical models of the electro-rheological response of liquid crystals have been developed by Negita[23] (a modified Leslie-Ericksen approach), and by Reyes et al.[25] (a hydrodynamic model of a nematic system confined in a rectangular cell).

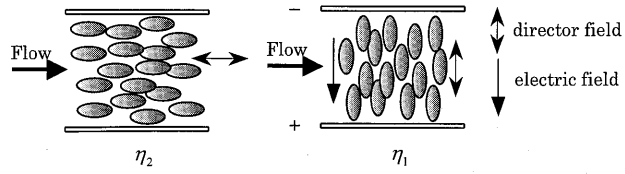

Fig. 1 Schematic mechanism of ER effect in liquid crystal ($\Delta\varepsilon > 0$). Note that the Miesowicz viscosities satisfy $\eta_1 > \eta_2$

This paper is structured as follows. The next section will detail the experimental materials, the apparatus and the procedure. Following that, the results and discussion will be presented, and finally there will be some concluding remarks.

2. Experimental

2.1 Materials

The liquid crystalline samples used were thermotropic types, which are in the nematic phase at the laboratory temperature of 20°C. These were kindly supplied by Chisso Petrochemical Corporation (Japan). We used four different liquid crystals of this same basic type, labeled as JD-1015XX, JD-1017XX, JD-1018XX and JD-1019XX. The key physical properties are presented in Table 1. JD-1015XX is the basic sample and JD-1017XX has large dielectric anisotropy $\Delta\varepsilon$. JD-1018XX and JD-1019XX have different average molecular aspect ratios compared to the basic one. The detailed chemical composition of these samples was proprietary information, and was not available. In this report, we will mainly focus on the ER property due to oscillatory flow and try to derive a model to describe the force - displacement response. Therefore, the influence of the different physical properties of liquid crystals will not be discussed here, and will be treated in a future publication.

2.2 Apparatus

Figure 2 shows schematically the oscillatory squeeze flow rheometer used in this study. This is a commer-

Table 1 Physical properties of liquid crystals used

	Dielectric Anisotropy $\Delta\varepsilon$	Viscosity (20℃) [mPa·s]	Average Molecular Aspect Ratio
JD-1015XX	4.7	23.8	3
JD-1017XX	8.6	31.5	3
JD-1018XX	3.8	17.4	2.7
JD-1019XX	5.1	39.6	3.3

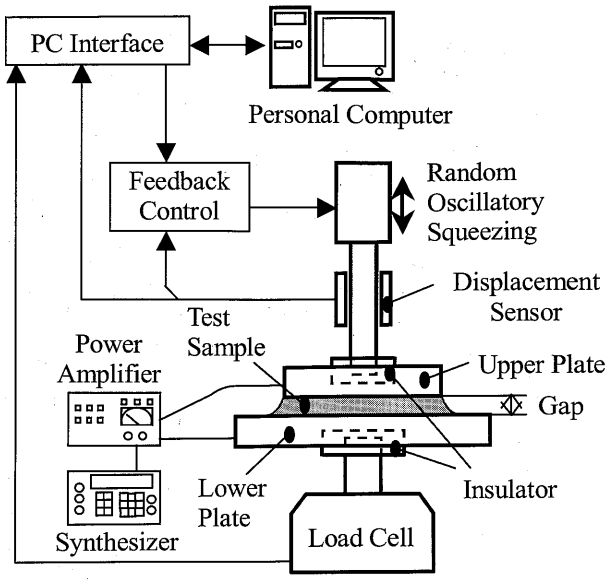

Fig. 2 Schema of experimental apparatus with Micro-Fourier Rheometer (MFR 2100)

cially available instrument, known as the Micro-Fourier Rheometer (GBC model MFR 2100), which has already been used to study a variety of viscoelastic materials[26)-28)]. Details of the essential construction and operation of the device have been presented elsewhere[26)], and so just a brief description of the main features will be presented here. The upper plate of the instrument is attached via a shaft to a vertical motion driver which in turn was connected to a signal generator with feedback. The oscillatory output motion (up to 200π rad/s) was linearized using a PID feedback controller. The instantaneous vertical position of the upper plate was detected by a fiber-optic device, giving the displacement $h(t)$. The amplitudes of the oscillatory motions were kept small to explore the linear viscoelastic properties of the sample. The bottom plate remained stationary, and a piezoelectric load cell rigidly attached underneath was used to measure the instantaneous force $F(t)$. Analog signals from the load cell are digitized using analog to digital converters (ADC). These were synchronized with the signals from the position detection system and the digital values were used by the computer software. Thus, in summary, the essence of the technique is that a known vertical displacement $h(t)$ is applied to the sample via the upper plate, and the resistance force arising from the sample $F(t)$ is measured by the load cell.

The key equation for this technique, relating $F(t)$ to $h(t)$, is based on the Stefan equation for the compression of a fluid between parallel surfaces[29)] modified for the case of a viscoelastic material[26),30)]. If the input is the oscillatory displacement signal $h(t) = h_0 + \Delta h(t)$ and $\Delta h = \xi \cdot h_0 \exp(i\omega t)$ (strain amplitude ξ, mean gap value h_0, angular frequency ω), this equation gives the following for the amplitude of the instantaneous output force signal $F(t)$.

$$F(t) = \frac{3}{2}\frac{\pi a^4 \eta^*(\omega)}{h_0^3}(-\dot{h}) \tag{1}$$

where $\dot{h} = i\omega\xi \cdot h_0 \exp(i\omega t) = i\omega\Delta h$, or

$$F(t) = \frac{3}{2}\frac{\pi a^4 G^*(\omega)}{h_0^3}(-\Delta h(t)) \quad . \tag{2}$$

Here $G^*(\omega) = i\omega\eta^*(\omega)$, and $\eta^*(\omega) = \eta'(\omega) - i\eta''(\omega)$ is the complex viscosity. In the case of Newtonian fluid, the force will have an in-phase and 90° phase shifted component compared to the input sinusoid of Δh. The sample disk has a radius of a. Another useful quantity is the phase angle, δ, between F and Δh and is defined by $\delta = \tan^{-1}(\eta''/\eta')$. Equation (1) can be derived from first principles using the lubrication approximation - details will be omitted here (see Phan-Thien[29)] for the calculations). It is worth pointing out that the strain field in a sample under squeezing deformation is not uniform, but this has been accounted for in the analysis (at least within the framework of the lubrication approximation).

The explanation of the instrument and its operating principle presented so far has been for a single angular frequency ω. We will now briefly discuss the principle of estimation of complex viscosity from the random oscillatory squeezing. Since this is a small strain test and the material is responding in the linear viscoelastic regime, the principle of linear superposition can be employed. This means that the input signal can actually be a superposition of sinusoids at different frequencies, and Fourier analysis of the output force signal will separate the contributions of the different frequency components. Indeed, pursuing this approach further, a band-limited pseudorandom noise can be used as the input displacement signal, whereby displacements at different frequencies are telescoped into a single synthetically generated excitation sequence. This instrument has this capacity, and the frequency range which can be covered is 4π to 200π rad/s with a resolution of π. Clearly the advantage of this method is that it provides a rapid and efficient method for determining $\eta'(\omega)$ and $\eta''(\omega)$ over a range of frequencies - this is much faster than carrying out individual tests at each frequency over the same range. In these experiments, we will express our results using the modulus of complex

viscosity $|\eta^*| = \sqrt{\eta'^2 + \eta''^2}$, which indicates the overall resistance to deformation, and δ, which indicates the phase behaviour.

In our tests, the typical gap h_0 was 0.25 mm and the characteristic strain amplitude ξ was 0.4%, giving us an oscillation amplitude $\xi \cdot h_0$ of 1 μm. The upper plate radius (a) was 10.5 mm. Further, as shown in Fig. 2, this instrument was modified to apply an AC electric field of frequency 1 kHz to the sample across the plates. This was applied using a power source (NF Corp., type 4020). Since the amplitude of the oscillations is small compared to the mean gap, the amplitude of the electric field signal can be thought of as essentially constant. We confirmed that the samples were responding in the linear viscoelastic regime by examining the resulting force waveforms - these were indeed sinusoidal and the force amplitude was proportional to the oscillatory strain amplitude applied.

3. Results and Discussion

3.1 ER effect in oscillatory squeeze flow

Figure 3 (a) and (b) show the response for JD-1015XX sample. Figure 3 (a) shows the modulus of the complex viscosity $|\eta^*|$, which is used to characterize the stiffness of the material. The values have been normalized with respect to η_0 which is the steady shear viscosity in the absence of an electric field (measured using a conventional cone-plate rheometer – Haake RS-50). Figure 3 (a) shows the variation of $|\eta^*|$ with oscillation frequency and electric field strength is plotted. We see that, as field strength is raised, there is an increase in the viscosity levels across the frequency range. Further, we find that for a fixed field, there is a decrease in viscosity with increasing frequency. These tendencies are very similar to those observed in the steady shear ER response of liquid crystals: that is, the shear viscosity decreases with increasing shear rate[31]. However, in our tests, a peculiar phenomenon in the ER effect is observed in the high shear region under lower electric fields. We see that the quantity $|\eta^*|/\eta_0$ decreases to a constant value regardless of the electric field strength with increasing shear rate, and that it takes values less than 1. Interestingly, for comparison, the viscosity measured under no electric field shows values larger than 1. More directly, we have examined the force amplitude (F_p) at constant frequency, as shown in Fig. 4. We see the force amplitude actually decreases for fields up to 200 V/mm and then increases for larger fields: that is, a negative ER effect was obtained under low electric field. From a practical viewpoint, this means that we are able to closely control the force amplitude from lowest case to the highest case. So, hereafter, when we quantify the ER effect, we will take the ratio against the lowest value, η_0^* (see Fig. 7 for the definition), and we note that this value is constant for the higher electric fields. At this stage, we do not know the mechanism behind the negative ER effect

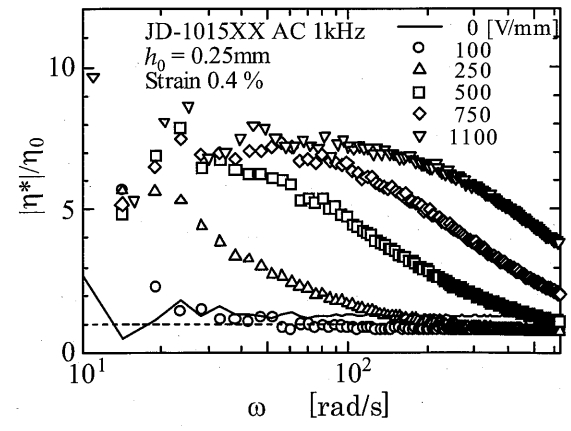

(a) Complex viscosity

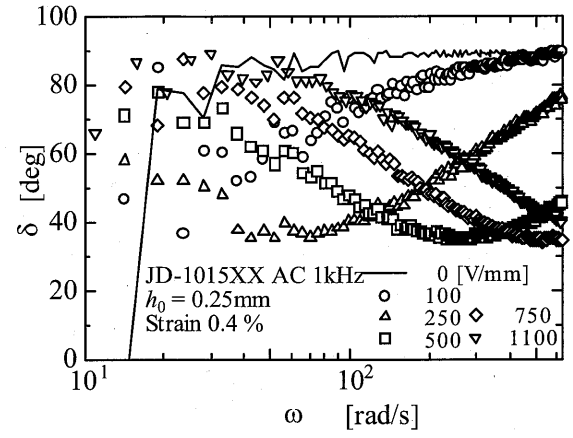

(b) Phase shift angle

Fig. 3 Complex viscosity and phase shift angle of JD-1015XX under AC electric fields measured with MFR

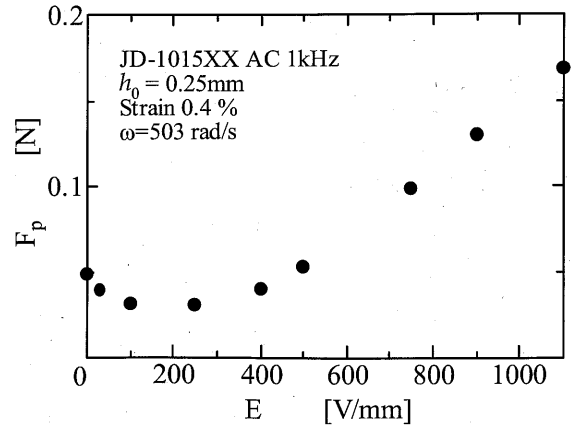

Fig. 4 Force amplitude obtained with a constant frequency (80 Hz)

and the reason why η_0^* is not just the value η_0 from steady flow. We speculate that the motion of the liquid crystal molecules, to be discussed below, would be an important factor for these phenomena.

In Fig. 3 (b), the frequency and electric field dependence of the phase angle δ is shown, and we see that there is a clear dip in δ at intermediate frequencies, indicating

an elastic component of the response. This dip in δ shifts to higher frequencies as the field strength is raised. Curves with similar shapes were obtained for the four other samples, but will be omitted here to avoid repetition. The reduction in δ means that liquid crystals show viscoelasticity depending on the electric field strength and frequency of oscillatory flow. It should be noted that this is not an intrinsic material property, as these phenomena arise from the molecular motion due to the electric and shear forces applied. Hence, this phase shift would be expected to have a correlation with the response of the liquid crystal to the electric field. Thus, we introduce a response time t_r, which describes how quickly the director aligns when an electric field is applied[32]. The time t_r depends on $\Delta\varepsilon$ and electric field strength E as follows:

$$t_r = \eta_i / \left(\varepsilon_0 \cdot |\Delta\varepsilon| \cdot E^2\right) \tag{3}$$

Here η_i is a characteristic viscosity - we will use the viscosity η_e^* (cf. Fig. 7) measured in the low frequency region under the electric field, because all tests are conducted under electric field. ε_0 is the permittivity of space ($\varepsilon_0 = 8.55 \times 10^{-12}$ F/m). The characteristic times t_r evaluated at $E = 500$ V/mm for all samples are listed in Table 2. This prompts us to re-plot the response curves in Fig. 3 (a) and (b) using a rescaled frequency axis $\omega \cdot t_r$. This is shown in Fig. 5 (a) and (b), and we observe that there is indeed good data collapse across most of the frequency range. It thus seems that the relaxation phenomenon observed in the viscoelastic tests is closely related to the electric response time (t_r). The data collapse when the frequency dependence of the viscoelastic functions are re-plotted with $\omega \cdot t_r$ is similar to the collapse observed in particulate electrorheological fluids[14),(15)], although the relaxation mechanism is quite different (rearrangement of particles within the aggregates for the particulate systems).

It is clear from Fig. 5 (b) that the liquid crystals under electric fields tend to show close-to-purely-viscous behaviour at low and high frequencies (the phase angle is approaching 90°), and an increasing elastic component at intermediate frequencies (around $\omega \cdot t_r \approx 5$). We now briefly present a possible physical explanation for this behaviour (Fig. 6 (a)–(c)). At low frequencies, the characteristic shear rates are small, and so there is not a large moment acting on the molecules to perturb them from the aligned configuration (Fig. 6 (a)). Although this configuration would cause a large viscosity, the fact that the molecules do not exert a substantial net moment on the fluid themselves means that the bulk of the mechanical resistance is associated with a viscous–type response, with only a small elastic component (i.e. the viscosity is high in Fig. 5 (a), with δ close to 90°). At intermediate frequencies (Fig. 6 (b)), the moment arising from the flow field is larger, and thus the molecules tend to be more perturbed from the aligned state. There is a torque acting on these due to the electric field, which attempts to align the molecules in the field direction – this would tend to contribute an elastic or in-phase component to the response (hence δ is significantly less than 90°). Overall, since the molecules are less aligned with the field direction, there would be a reduced resistance to flow, which could correspond to the decrease in $|\eta^*|$ observed in Fig. 5 (a). Finally, at high frequencies, the torque from the flow field is large enough to align the molecules in the flow direction (Fig. 6 (c)) – in this case the flow resistance is minimal (low $|\eta^*|$) and the mechanical response is again close to purely viscous behaviour.

Table 2 Characteristic times and model constants (AC1 kHz, 500 V/mm[1)])

	JD-1015XX	JD-1017XX	JD-1018XX	JD-1019XX
t_r [s] [1)]	1.74E-02	0.91E-02	1.08E-02	3.40E-02
T [s] [1)]	1.22E-03	0.968E-03	1.18E-02	1.91E-03
k (η_e^*) [Pa·s]	0.175	0.167	0.088	0.37
α (η_e^*/η_0^*)	9.99	6.50	6.78	12.4

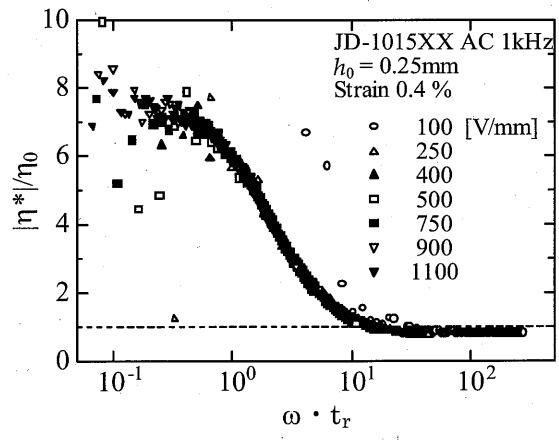

(a) Complex viscosity

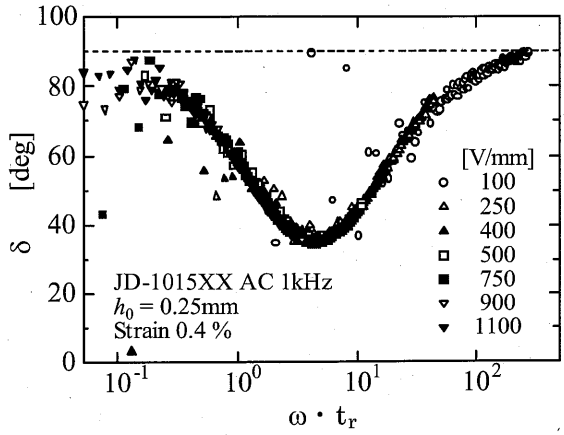

(b) Phase shift angle

Fig. 5 Master viscosity curves obtained using the characteristic time

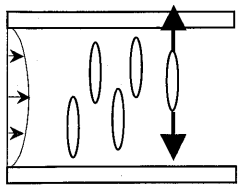

(a) Low frequency ($\omega \cdot t_r \ll 1$)

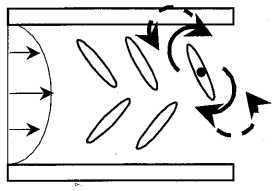

(b) Intermediate frequency ($\omega \cdot t_r \sim 1$)

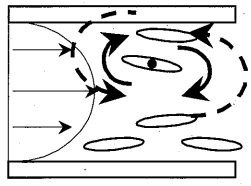

(c) High frequency ($\omega \cdot t_r \gg 1$)

: Moment due to shear field

: Moment due to electric field

Fig. 6 Schematic images of molecular motion of liquid crystal subject to oscillatory shear flow and electric field

3.2 Rheological model and transfer function

As discussed above, we have considered that this pseudo-elasticity, i.e. the phase shift, is due to the delayed response of the liquid crystal director. The application of this ER material in any engineering device would require some kind of control system, and so, based on the results found above, it would be useful to have a rheological expression between the input Δh and the output F that can also estimate the phase shift (i.e. a transfer function). Here, we will recast the governing Eq. (2) into a form useful for control theory. Rearranging Eq. (2), we obtain

$$\frac{F(t)}{\Delta h(t)} = -\frac{3}{2}\frac{\pi a^4}{h_0^3} G^*(\omega) = -A \cdot G^*(\omega) \tag{4}$$

Since $A = 3\pi a^4 / 2h_0^3$ is a constant, we can regard $G^*(\omega)$ as essentially a transfer function between Δh and F in an oscillatory motion. δ in Fig. 3 (b) or 5 (b) shows that these responses are very similar to those obtained with a phase lag element and a derivative element in control theory. Hence we will assume the following expression:

$$G^*(i\omega) = k\frac{i\omega T + 1}{i\omega T\alpha + 1} \cdot i\omega, \tag{5}$$

where k, T, α are constants in the transfer function. Then, using $G^*(\omega) = i\omega\eta^*(\omega)$, we have the magnitude of complex viscosity as,

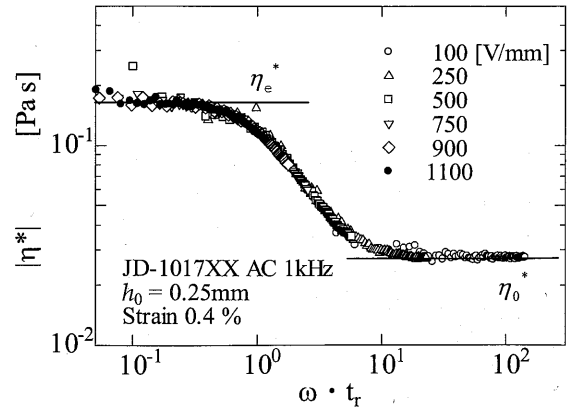

Fig. 7 Definition of η_0^* and η_e^*

$$\eta^* = k\frac{i\omega T + 1}{i\omega T\alpha + 1} \quad \text{or in magnitude;} \quad |\eta^*| = k\left|\frac{i\omega T + 1}{i\omega T\alpha + 1}\right| \tag{6}$$

Therefore, as shown in Fig. 7, the constants are easily related to the physical properties, as follows:

$$\lim_{\omega \to 0} |\eta^*| = k = \eta_e^* \tag{7}$$

$$\lim_{\omega \to \infty} |\eta^*| = \frac{k}{\alpha} = \eta_0^* \tag{8}$$

$$\alpha = \frac{\eta_e^*}{\eta_0^*} \tag{9}$$

Hence, α represents the magnitude of the ER effect, i.e. the increase in viscosity. It should be noted that these constants are independent of E. Moreover, both η_e^* and η_0^* are obtained in limit to Newtonian region, so that they have a real part only. Since T in Eq. (5) is a characteristic time in the transfer function, it would be useful to examine the correlation between this time and the time t_r, which was discussed earlier. We see from Fig. 8 that there is good correspondence between t_r and αT: indeed, as Fig. 8 suggests, it seems that $\alpha T = ct_r$ where c is an empirical constant $c = 0.71$. Although Fig. 8 is obtained at $E = 500$ V/mm, the value of c was found to be essentially independent of the electric field strength. In summary, the model constants for all samples are shown in Table 2, with T being the value at 500 V/mm. Hence we can express the complex viscosity with physical constants as follows:

$$\eta^* = \frac{i\omega\eta_0^* \cdot ct_r + \eta_e^*}{i\omega \cdot ct_r + 1} \tag{10}$$

Finally, the phase shift angle δ is easily calculated utilizing Eq. (5) or (10). Here we simply express it as follows;

$$\delta = \angle G^*(i\omega) \tag{11}$$

A typical comparison between the data measured and Eqs. (10) and (11) is shown in Fig. 9 (a) and (b) for JD-1019XX. We see that the models are able to estimate reasonably well the "output response" of the ER effect, namely the viscosity increase and the phase shift. Thus, we see that Eqs. (10) and (11) are reasonable rheological

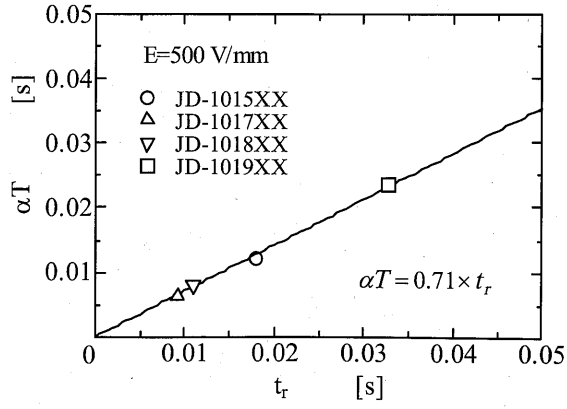

Fig. 8 Correlation between the two characteristic times, T and t_r

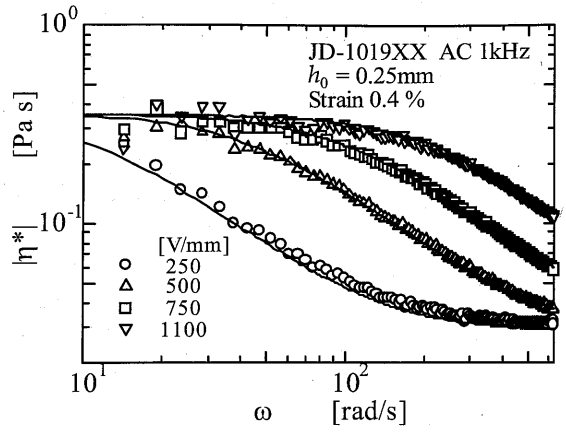

(a) Complex viscosity

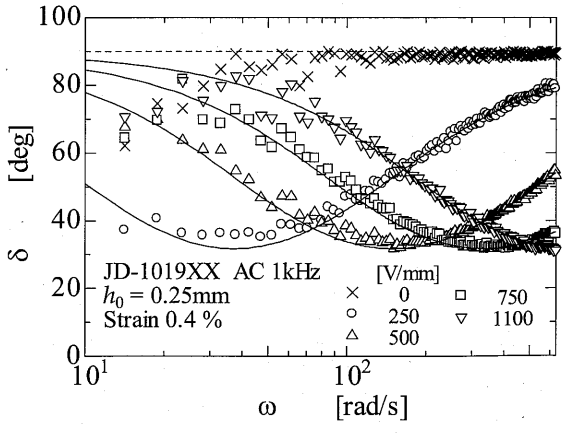

(b) Phase shift angle

Fig. 9 Comparison between experimental data and the rheological model derived

models for the liquid crystal incorporating viscoelasticity under electric fields, and moreover these equations also give us a transfer function useful for the flow or motion control.

4. Concluding Remarks

A measurement of the electric field-induced viscoelastic properties of liquid crystalline samples has been carried out using an oscillatory squeeze flow instrument. A clear dip in the phase angle centred around a frequency which increased with electric field strength was observed. It was found that this critical frequency was proportional to the inverse of the response time required for the liquid crystal molecules to align under the electric field. The ER effect observed in the oscillatory flow was similar to that under steady flow; that is, the increased Newtonian viscosity at low frequency is independent of the electric field strength, and the viscosity decreases as frequency is raised. However, it was found that the value at high frequency was smaller than that under no electric field. In other words, we obtained a negative ER effect under low electric fields, i.e. the fluidity is slightly increased under an electric field. A rheological model for the dynamic response was obtained through control theory. The model parameters were determined with the physical properties of the liquid crystal under electric field. This model should prove useful as the transfer function to estimate the output response in a flow or motion control system.

Electrorheological technology based on liquid crystalline materials continues to be developed, but up to now there have been no reports of the viscoelastic response, which, as we have seen, can reveal much about the dynamic behaviour. One area to be explored in future work would be to apply a range of frequencies of the AC electric field and to observe what happens when the frequency of the field approaches that of the oscillatory deformation - matching of these frequencies could lead to interesting 'resonance' effects. There is clearly scope for much further investigation into the dynamic behaviour of liquid crystalline electrorheological materials - the intriguing scientific issues and the wide range of potential engineering applications of these materials make them an exciting and challenging field for rheologists.

Acknowledgements

The authors gratefully acknowledge the assistance of Mr. Koichi Fujita (Hitachi High-Tech Trading Corporation) for giving us the opportunity to use the Micro-Fourier Rheometer, as well as the help of Mr. Takashi Nanbu in the experimental stages of this project. We would also like to thank Dr. Kazutoshi Miyazawa et al. (Chisso Petrochemical Corporation) for kindly providing the liquid crystal samples.

References

(1) Jordan, T. and Shaw, M., Electrorheology, IEEE Trans. Elect. Insul., Vol.24 (1989), pp.849–878.

(2) Parthasarthy, M. and Klingenberg, D.J., Electro-Rheology: Mechanisms and Modeling, Mat. Sci. Eng., Vol.R 17 (1996), pp.57–103.

(3) See, H., Advances in Modelling the Mechanisms and Rheology of Electrorheological Fluids, Korea Australia Rheology Journal, Vol.11 (1999), pp.169–195.

(4) Narumi, T., Maeda, H., Hasegawa, T. and Sakai, M., Electrorheological Effect of Liquid Crystals in Narrow Gaps, Proc. JSME ICFE '97, Vol.1 (1997), pp.497–500.

(5) Narumi, T., Yoshizawa, H. and Hasegawa, T., Rheological Characteristics of Liquid Crystals in Narrow Gaps under Electric Field, Proc. 8th Australian National Conference on Rheology, (1998), pp.169–172.

(6) Morishita, S., Matsumura, Y. and Shiraishi, T., Oil Film Thickness Control of a Sliding Bearing Using Liquid Crystal as Lubricant, (in Japanese), J. Japanese Society of Tribologists, Vol.47, No.11 (2002), pp.846–851.

(7) Takesue, N., Furusho, J. and Inoue, A., Electrorheological Effects of Liquid Crystalline Polymer on One-Sided Pattern Electrodes, J. Appl. Phys., Vol.91 (2002), pp.1618–1623.

(8) Takesue, N., Furusho, J. and Inoue, A., Influence of Electrode Configuration and Liquid Crystalline Polymer Type on Electrorheological Effect, J. Appl. Phys., Vol.94 (2003), pp.5367–5373.

(9) Inoue, A., Ryu, U. and Nishimura, S., Caster-Walker with Intelligent Brakes Employing ER Fluid Composed of Liquid Crystalline Polysiloxane, Proc. 8th Int. Conf. on Electrorheological Fluids and Magnetorheological Suspensions, (2001), pp.23–29.

(10) Orihara, H., Ikeyama, Y., Ujiie, S. and Inoue, A., Observations of Immiscible Polymer Blend Electrorheological Fluids with a Confocal Scanning Laser Microscope, J. Rheology, Vol.47 (2003), pp.1299–1310.

(11) Tajiri, K., Orihara, H., Ishibashi, Y., Doi, M. and Inoue, A., Transient Response of Electrorheological Effect to a Step Field in an Immiscible Polymer Blend: Second Mode in Type I Blend, J. Rheology, Vol.43 (1999), pp.137–146.

(12) Kimura, H., Aikawa, K., Masubuchi, Y., Takimoto, J., Koyama, K. and Uemura, T., 'Positive' and 'Negative' Electro-Rheological Effect of Liquid Blends, J. Non-Newtonian Fluid Mech., Vol.76 (1998), pp.199–211.

(13) Klingenberg, D.J., Simulation of the Dynamic Oscillatory Response of Electro-Rheological Suspensions: Demonstration of a Relaxation Mechanism, J. Rheology, Vol.37 (1993), pp.199–214.

(14) Parthasarathy, M., Ahn, K., Belongia, B. and Klingenberg, D.J., The Role of Suspension Structure in the Dynamic Response of Electrorheological Suspensions, Proc. 4th Int. Conf. on Electro-Rheological Fluids, (1994), pp.202–222.

(15) Parthasarathy, M. and Klingenberg, D.J., Large Amplitude Oscillatory Shear of ER Suspensions, J. Non-Newtonian Fluid Mech., Vol.81 (1999), pp.83–104.

(16) See, H., Field, J. and Pfister, B., The Response of Electrorheological Fluid under Oscillatory Squeeze Flow, J. Non-Newtonian Fluid Mech., Vol.84 (1999), pp.149–158.

(17) El Wahed, A., Sproston, J. and Stanway, R., The Performance of an Electrorheological Fluid in Dynamic Squeeze Flow under Constant Voltage and Constant Field, J. Phys D: Appl. Phys., Vol.31 (1998), pp.2964–2974.

(18) El Wahed, A., Sproston, J. and Stanway, R., The Performance of an Electrorheological Fluid in Dynamic Squeeze Flow: The Influence of Solid-Phase Size, J. Colloid and Interface Sci., Vol.211 (1999), pp.264–280.

(19) El Wahed, A., Sproston, J. and Williams, E., The Effect of a Time-Dependent Electric Field on the Dynamic Performance of an Electrorheological Fluid in Squeeze, J. Phys D: Appl. Phys., Vol.33 (2000), pp.2995–3003.

(20) Kim, D., Chu, S., Ahn, K. and Lee, S., Dynamic Simulation of Squeezing Flow of ER Fluids Using Parallel Processing, Korea Australia Rheology Journal, Vol.11 (1999), pp.233–240.

(21) Lacey, D., Malins, C., Taylor, P., Hosseini-Sianaki, A. and Varley, C., Investigation into the Use of Liquid Crystalline Materials in Electrorheological Fluids, J. Intell. Mater. Sys. Struct., Vol.7 (1996), pp.526–529.

(22) Yao, N. and Jamieson, A., Electrorheological Creep Response of Tumbling Nematics, J. Rheology, Vol.42 (1998), pp.603–619.

(23) Negita, K., Electrorheological Effect Observed in the Nematic Phase of 4-n-pentyl-4'-cyanobiphenyl, J. Chem. Phys., Vol.17 (1996), pp.7837–7841.

(24) Miesowicz, M., The Three Coefficients of Viscosity of Anisotropic Liquids, Nature, Vol.158 (1946), p.27.

(25) Reyes, J., Manero, O. and Rodriguez, R., Electrorheology of Nematic Liquid Crystals Uniform Shear Flow, Rheol. Acta, Vol.40 (2001), pp.426–433.

(26) Field, J., Swain, M. and Phan-Thien, N., An Experimental Investigation of the Use of Random Squeezing to Determine the Complex Modulus of Viscoelastic Fluids, J. Non-Newtonian Fluid Mech., Vol.65 (1996), pp.177–194.

(27) See, H., Jiang, P.and Phan-Thien, N., Concentration Dependence of the Linear Viscoelastic Properties of Particle Suspensions, Rheol. Acta, Vol.39 (2000), pp.131–137.

(28) Jiang, P., See, H., Swain, M. and Phan-Thien, N., Using Oscillatory Squeezing Flow to Measure the Viscoelastic Properties of Dental Composite Resin Cements during Curing, Rheol. Acta, Vol.42 (2003), pp.118–122.

(29) Stefan, J., Akad. Wiss. Math. Wien Sitzungsber, Vol.69 (1874), p.713.

(30) Phan-Thien, N., Small Strain Oscillatory Squeeze Film Flow of Simple Fluids, J. Aust. Math. Soc., Ser. B, Vol.32 (1980), pp.22–27.

(31) Narumi, T., Sugahara, K., Hasegawa, T. and Igarashi, R., ER Effect of Liquid Cryastals Affected with Its Some Properties and Surface Alignment Treatment in Narrow Gaps, (in Japanese), Proc. 27th Annual Meeting of the Society of Rheology, Japan, (2000), pp.113–114.

(32) Matsumoto, S. and Tsunoda, I., Liquid Crystals–Fundamentals and Applications, (in Japanese), (1991), pp.89–90, Kogyo Chosakai Pub. Co., Ltd.